Axinite-(Mn) from miarolitic granitic pegmatites of the Malkhan gem-tourmaline deposit (Transbaikalia, Russia): Composition, paragenesis and conditions of formation

Article *in* European Journal of Mineralogy · June 2016

DOI: 10.1127/ejm/2016/0028-2544

CITATIONS
7

READS
710

3 authors, including:

Igor S. Peretyazhko
Vinogradov Institute of Geochemistry SB RAS
108 PUBLICATIONS **775** CITATIONS
SEE PROFILE

A.s. Dmitrieva
Институт геохимии им. Виноградова СО РАН, Иркутск
8 PUBLICATIONS **17** CITATIONS
SEE PROFILE

Eur. J. Mineral.
2016, **28**, 811–824
Published online 6 June 2016

Axinite-(Mn) from miarolitic granitic pegmatites of the Malkhan gem-tourmaline deposit (Transbaikalia, Russia): composition, paragenesis and conditions of formation

VICTOR YE. ZAGORSKY†, IGOR S. PERETYAZHKO* and ANNA S. DMITRIEVA

Institute of Geochemistry SB RAS, 1a Favorsky str., Irkutsk 664033, Russia
*Corresponding author, e-mail: pgmigor@igc.irk.ru
†Deceased 14 May 2015

Abstract: Axinite is an exotic accessory mineral in granitic pegmatites because conditions favorable for its formation are seldom reached. The compositional ranges of axinite from granitic pegmatites are close to the axinite-(Mn) and the axinite-(Fe) end-members. We report data on the composition of axinite-(Mn) and the formation conditions of axinite-containing mineral assemblages in miarolitic granitic pegmatites of the Malkhan gem-tourmaline deposit. Axinite-(Mn) occurs only in the pockets in which Li-Al tourmaline (rubellite) is either absent or transformed into an aggregate of asbestiform tourmaline. Axinite-(Mn) is associated with quartz, orthoclase, adularia and laumontite. The pockets may also contain dark, corroded Mn-Li-Al tourmaline and colorless or pale-pink beryl. The mineral association with axinite-(Mn) was formed from low-salinity (1.6–10.5 wt% NaCl-eq.), B-rich fluids (up to 13 wt% H_3BO_3) of high alkalinity in the temperature interval from < 415°C (maximum temperature of adularia formation) to <250–230°C (upper limit of laumontite stability) and at less than 1.5 kbar fluid pressure. The axinite-(Mn) contains high concentrations of BeO (0.58–0.69 wt%) and the main trace elements are REE, Sn, Nb, Ta, Hf, Th and U. The axinite-(Mn) + adularia ± laumontite association is an indicator of unfavorable conditions for the occurrence of gem tourmalines in miarolitic granitic pegmatites.

Key-words: Malkhan gem tourmaline deposit; miarolitic granitic pegmatite; axinite-(Mn); asbestiform tourmaline; orthoclase; adularia; laumontite; fluid inclusions.

1. Introduction

Minerals of the axinite group are the most widespread borosilicates in natural environments after tourmaline and dumortierite (Ozaki, 1972; Grew, 1996; Deer *et al*., 1997). The general formula of axinite was defined as $(Ca,Mn)_4(Fe,Mn,Mg)_2Al_4B_2Si_8O_{30}(OH)_2$ (Sanero & Gottardi, 1968). The formula was later modified to account for the cation distribution in the structural sites: $^{VI}[(Mn,Fe^{2+},Mg,Zn,Al_w)(Ca_{2-x}Mn_x)(Al_{2-y}Fe^{3+}{}_y)]_2(OH_{2-w}O_w)[^{IV}(B_2Si_{8-z}Al_z)O_{30}]$, where $w < 1$, $x < 1$, $y \ll 1$, $z \ll 1$, and VI and IV represent the cation coordination (Lumpkin & Ribbe, 1979). Andreozzi *et al*. (2004) further suggested a similar but more precise formula of cation distribution in the structural sites: $^{VI}[X1,X2,Y,Z1,Z2]_2\ ^{IV}[T1,T2,T3,T4,T5]_2\ O_{30}(O_wOH_{1-w})_2$, where X1 = Ca and minor Na; X2 = Ca and Mn^{2+}; $Y = Fe^{2+}$, Mn^{2+}, Mg with minor Al, Fe^{3+}, Zn; Z1 = Al and Fe^{3+}; Z2 = Al; T1-T3 = Si; T4 = Si and presumably minor B; T5 = B and minor Si. Charge unbalance (w), due to heterovalent substitutions, is compensated by $O^{2-} \rightarrow OH^-$ substitution.

The nomenclature of axinite-group minerals is based on the ratio of divalent octahedrally coordinated cations (Ca, Fe, Mn or Mg) located in the X and Y sites (Sanero & Gottardi, 1968; Lumpkin & Ribbe, 1979; Grew, 1996; Belokoneva *et al*., 2001; Andreozzi *et al*., 2004; Filip *et al*., 2006). Four end-members of the axinite group are axinite-(Fe), axinite-(Mn), axinite-(Mg) with 4 Ca atoms per formula unit (*apfu*) in the X site and dominant Fe, Mn or Mg in the Y site; and tinzenite with $2 \leq Ca \leq 4$ *apfu* and dominant Mn at both the X2 and Y sites. The minerals with Ca ~ 3–4 *apfu* and Mn ~ 2–3 *apfu* are often referred to as 'severginite' and 'manganseverginite' or low-Mn tinzenite, respectively, in Russian-language publications (Barsanov, 1961; Kurshakova, 1968; Minerals, 1981; Belokoneva *et al*., 1997). The compositional range of most axinite-group minerals extends along the solid solutions axinite-(Mn)–axinite-(Fe) and axinite-(Mn)–tinzenite, with a compositional gap between axinite-(Mn) and axinite-(Mg) (Grew, 1996; Andreozzi *et al*., 2000).

Axinite is commonly found in metasomatites associated with the deposits of tin, copper, manganese, base metals, magnetite and with mineralization products of skarn deposit (Minerals, 1981). Minor amounts of axinite were found sporadically in cavities of the Alpine-type veins, *e.g*. in the Polar Urals (Bukanov, 2014) and the type area. Axinite was also discovered in miarolitic

DOI: 10.1127/ejm/2016/0028-2544
0935-1221/16/0028-2544 $ 6.30

pockets from intragranitic pegmatites of Waldstein granites, Fichtelgebirge, Bavaria, Germany and Striegauer granites (Strzegom-Sobótka massif), Strzegom, Lower Silesia, Poland (Fersman, 1960; Janeczek, 2007). Fine crystals of brown axinite-(Mn) up to 0.5 mm size overgrowing quartz and feldspar crystals were found in pockets of the Baveno (Italy) alkaline pegmatites (Albertini, 1983). The largest crystals of axinite-(Mn) of 2.5 × 5 cm size were described in pockets of the Little Three pegmatites (Dykes Spolding, Hutfield Creek, Hercules-Spessartine) in California, USA (Foord *et al*., 1989). The axinite-(Mn) crystals in the Little Three pegmatites had differentially corroded faces associated with black tourmaline, K-feldspar, albite and spessartine. Axinite-containing pockets were also discovered during development of the Sosedka pegmatite body at the Malkhan gem-tourmaline deposit, Transbaikalia, Russia (Zagorsky & Peretyazhko, 2008). The objectives of our study were to characterize the composition of axinite-(Mn) and to determine formation conditions of axinite-containing mineral assemblages in the miarolitic granitic pegmatites of Malkhan deposit. We applied various methods of analysis (wet chemistry, ISP-MS, X-ray diffraction and optical microscopy) to characterize bulk samples of axinite-(Mn) and primary fluid inclusions in the pocket minerals.

2. Methods

For wet chemical analysis of major oxides, about 1 g of pure and transparent grains of axinite-(Mn), 0.1–0.5 mm in size, was selected from four crushed samples under binocular microscope. Trace elements in the axinite-(Mn), quartz, tourmaline, K-feldspar and laumontite were determined from up to 50 mg mineral samples by ICP-MS using NexION300D (Agilent Technologies Inc.) quadrupole mass spectrometer at the Institute of Geochemistry (IGC), Siberian Branch of the Russian Academy of Sciences (SB RAS).

Unit-cell parameters of axinite-(Mn) were determined by X-ray diffraction using D8 ADVANCE Bruker diffractometer with Cu*K*α radiation equipped with a Göbel mirror and VÅNTEC-1 PSD detector with radial Soller slits on the diffraction beam (IGC SB RAS, Irkutsk). The data were recorded in a step scan mode within the range 5° to 70° 2θ at 45 kV-40 mA with a 0.02° 2θ step for 1 s. The unit-cell parameters were refined using TOPAS 4 software (Bruker AXS, 2008).

Microthermometric observation of fluid inclusions (FI) in quartz, tourmaline, K-feldspar, beryl and axinite-(Mn) was performed with an Olympus BX-51optical microscope equipped with a Linkam THMSG-600 thermal/freezing stage, Pixelink video camera and LinkSys 32-DV temperature control and data capture software system (IGC SB RAS, Irkutsk). The thermal/freezing stage was calibrated using melting points of CO_2 in synthetic CO_2-bearing Linkam FI and solid $K_2Cr_2O_7$. The measurement error was ±0.01°C for <0°C, ±1°C for 0–400°C, and ±3°C for 400–600°C temperature ranges. Sassolite (H_3BO_3) in FI was identified by optical properties (Peretyazhko *et al*., 2000) and Raman spectroscopy with X-Y Dylor OMARS69 multichannel spectrometer (Institute of Geology and Mineralogy SB RAS, Novosibirsk). The concentration of boric acid (C_{H3BO3}) and salinity (NaCl-eq.) in fluids was estimated using H_2O–H_3BO_3–NaCl phase diagrams, temperatures of sassolite dissolution and ice melting (Peretyazhko *et al*., 2000, 2004a). The fluid density and pressure for the H_2O–H_3BO_3 system were defined by the method described in Peretyazhko & Zagorsky (2002) and Peretyazhko *et al*. (2004a). The fluid pressure of boric acid solution without CO_2 under isochoric conditions was calculated with the following equations:

$$P = P_{1-v} + (300 - T_{hom})dP/dT_{100-300°C} + (T - 300)\, dP/dT_{300-500°C} (T_{hom} < 300°C)$$

$$P = P_{1-v} + (T - T_{hom})dP/dT_{300-500°C} (T_{hom} > 300\,°C),$$

where T is the temperature for which pressure is calculated, T_{hom} is the homogenization temperature, $P_{1\text{-}v}$ the pressure at homogenization temperature, and dP/dT (bar/°C) the correction to temperature for the T_{hom} interval, equal to either 100–300°C or 300–500°C (Peretyazhko *et al*., 2004a).

3. Geological setting and inner structure of the Sosedka pegmatite body

The Malkhan gem-tourmaline deposit (Transbaikalia) is located within the metamorphic country rocks between the Bolsherechensky and Oreshny massifs of subalkaline biotite and two-mica granite-leucogranites (Zagorsky & Peretyazhko, 1992; Miarolitic Pegmatites, 1999). The deposit is hosted by Early Paleozoic orthogneisses of the Malkhan complex dominated by metadiorites. The measured $^{40}Ar/^{39}Ar$ ages of granites and pegmatites are 127–123 Ma (Zagorsky & Peretyazhko, 2010). Detailed descriptions of the geological setting, composition and inner structure of the Malkhan gem-tourmaline deposit and Sosedka pegmatite body in particular were given by Zagorsky & Peretyazhko (1992, 2008), Miarolitic Pegmatites (1999) and Zagorsky (2012, 2015).

The Sosedka pegmatite body is stripped by a continuous surface clearing and its southwestern and northeastern parts are mined by quarries. The steeply dipping oval-shaped pegmatite body is 80 × 50 m in size and has a concentrically zoned structure (Zagorsky & Peretyazhko, 2008; Zagorsky, 2015). The external ring zone ranges in width from 0–3 to 18–20 m. External and internal zones differ in mineral composition and pegmatitic textures. The external ring zone is composed of schorl-bearing quartz–oligoclase pegmatite of coarse-grained graphic or, more commonly, poorly developed graphic textures. The

average amount of schorl (cone-like crystals up to 5–7 cm in length) is around 1–3 vol% in the zone, but reaches 5–7 vol% in some locations. The quartz–oligoclase pegmatite of the thick external zone in the southwestern part of the Sosedka body contains "floating" spherical or egg-like schorl-free quartz–K-feldspar segregations of coarse-graphic and/or graphic textures. Segregations are usually less than 1.5–2 m across and their amount increases towards the internal zone of the body. The internal zone is composed of schorl-free quartz–K-feldspar pegmatite of coarse-grained graphic and block textures. This zone also contains small areas of quartz–oligoclase schorl-bearing pegmatite which are similar in textures to pegmatite of the external zone.

All zones of the pegmatite body contain numerous miarolitic pockets ranging in volume from 10–20 cm^3 to 10–15 m^3. The pockets differ substantially by the amount of loose miarolitic filling material (from 5–10 to 90–100 % of the pocket volume), mineral composition, druse associations, quality and quantity of crystal raw material. Three types of pockets are distinguished by the pattern of predominant mineralization:

Type "A" – quartz–lepidolite–Li-Al tourmaline ± pollucite, hambergite, borocookeite (Zagorsky *et al*., 2003), boromuscovite, danburite;

Type "B" – quartz–adularia–axinite-(Mn) ± laumontite;

Type "C" – quartz or laumontite ± B-bearing cookeite – subtypes "C_1" and "C_2", accordingly.

Pockets of different type are typically spaced 0.5 to 2 m from each other. Irregularly distributed "A" type pockets are only found in the external part of the pegmatite body. The "B" and "C" type pockets occur in both external and internal zones. The pockets amount increases towards the internal zone. In the internal zone the "C" type pockets dominate and the number of "B" type pockets tends to increase with depth. The gem tourmaline is derived from the "A" type pockets only. The genetic reasons for the pattern of pocket distribution within the Sosedka pegmatite body and other pegmatite bodies of the Malkhan deposit are discussed by Peretyazhko *et al*. (2004a and b) Peretyazhko (2009, 2010) and Zagorsky (2010, 2012, 2015).

4. Paragenesis of axinite-(Mn)

The presence of mineral associations of axinite-(Mn), adularia and asbestiform tourmaline is a characteristic feature of the "B" type pockets. The late adularia generation of K-feldspar produces light-gray or colorless rims on the early orthoclase crystals and separate crystals in some locations. The boundaries between the early orthoclase generation and adularia rim are always distinct and sharp in zoned crystals of K-feldspar; however, adularia can also penetrate through cracks into the internal zone. A thin (1–3 mm) zone with numerous needles of dark-colored tourmaline occasionally occurs on the boundary between early orthoclase and adularia. Axinite-(Mn) produces separate flattened semi-transparent light-brown crystals up to 2.5 cm in length or druses overgrowing K-feldspar and smoky quartz crystals (Fig. 1a). Axinite-(Mn) crystals are often half or more immersed into the adularia rim (Fig. 1b). Occasionally separate adularia crystals are found to lie within axinite-(Mn) druses growing over early orthoclase (Fig. 1c).

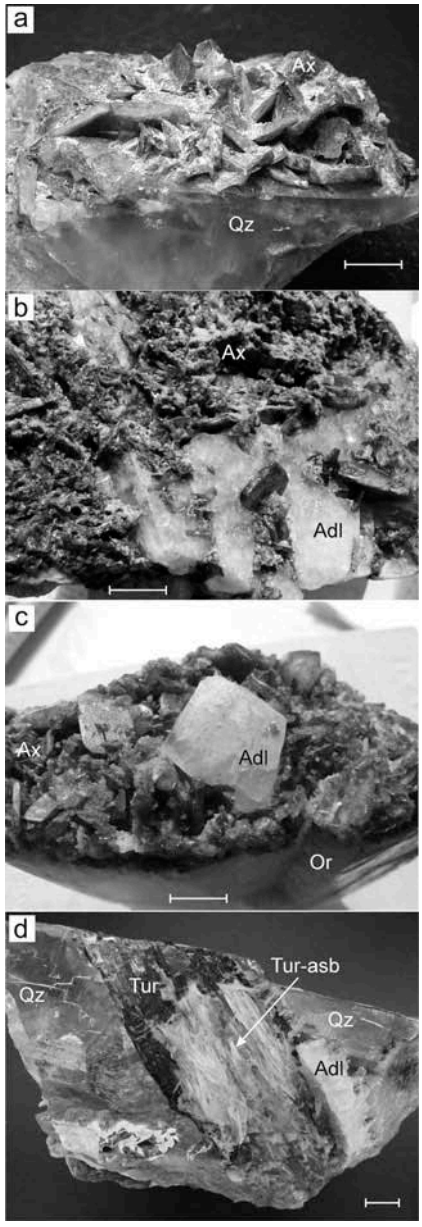

Fig. 1. Axinite-(Mn), adularia, quartz and tourmaline from "B" type pockets of the Sosedka pegmatite body.
a) Axinite-(Mn) crystals covers quartz; b) axinite-(Mn) and adularia crystals on the orthoclase; c) adularia and axinite-(Mn) crystals covering orthoclase; and d) partially replaced and recrystallized zoned tourmaline crystal in quartz with inner asbestiform tourmaline zone. Qz – quartz, Ax – axinite-(Mn), Adl – adularia, Tur – dark Mn-Li-Al-tourmaline, and Tur-asb – asbestiform tourmaline. Scale bar is 1 cm.

Tourmaline undergoes intense leaching and recrystallization in the "B" type pockets, leading to formation of asbestiform tourmaline (Fig. 1d). Tourmaline crystals are dark-brown or black with a completely or partially leached light-colored pinkish red internal zone. The partially replaced and recrystallized phase is pink Li-Al-tourmaline (rubellite) and the least altered phase is dark Mn-Li-Al-tourmaline forming the outer layer of zoned crystals. Numerous large crystals of quartz are encrusted with abundant small crystals of axinite-(Mn) and a few crystals of dark-brown tourmaline. In some cases the pockets contain crystals of pale pink beryl, 4 × 1.5 cm in size, embedded in quartz.

Axinite-(Mn) was also discovered within a narrow (10 to 25 cm wide) elongated zone amongst blocky K-feldspar at the depth of 6–7 m. This zone (called "steaming" zone after local miners) was formed under the action of fluid on the blocky K-feldspar. The fluid was released during the rupture of "B" type pockets and, perhaps, local degassing of residual melts. Leaching of K-feldspar is accompanied by formation of numerous vugs (micropockets) filled with a mixture of loose, fine-grained axinite-(Mn)–laumontite aggregates and quartz. The vug walls occasionally have K-feldspar overgrown with thin rims of semi-transparent adularia, and some vugs incorporate scarce needles of dark-brown tourmaline. The northwestern flank of the "steaming" zone borders the quartz–oligoclase pegmatite of the external zone. According to the classification of Zagorsky (2010), the pockets of the "steaming" zone are primary–secondary or pseudo-secondary.

5. Chemistry of the axinite from granitic pegmatites

Table 1 shows the chemical composition of axinite-group minerals from miarolitic granitic pegmatites of the Malkhan deposit, the Little Three mine (California) and pocket-free granitic pegmatites. The results reveal that axinite compositions from granitic pegmatites are close to the compositions of the axinite-(Fe) and axinite-(Mn) end-members on the ternary diagram Ca–Mn–(Fe^{2+},$Fe^{3+}_{(Y)}$,Mg) (Fig. 2). Compositions between axinite-(Mn) (Fe^{2+}+$Fe^{3+}_{(Y)}$ < 0.6 *apfu*) and axinite-(Fe) (Mn < 0.5 *apfu*) were not found in granitic pegmatites. Axinite-(Mn) from Malkhan and pocket-free granitic pegmatite in Minnesota have the highest content of Mn (Table 1, samples 4 and 7). All samples of axinite-(Mn) from the Malkhan deposit contain Be (0.27–0.32 *apfu*) and $Fe^{3+}_{(Y+Z)}$ (0.19–0.33 *apfu*) and show B deficit (0.30–0.47 *apfu)*. The lack of B in T positions is likely compensated by excess Si (0.08–0.32 *apfu*). The sum of B and Be in the structural formulas is close to 2 (1.796–2.006 *apfu*) in all samples from the Malkhan deposit. Three samples of axinite-(Mn) have $Fe^{3+}_{(Y+Z)}$ > Fe^{2+} (Table 1, samples 2–4).

Elevated Be content is likely a characteristic feature of axinites from granitic pegmatites. The axinite-(Mn) from Sosedka pegmatite body represented the first reported occurrence of axinite-(Mn) with substantial BeO contents (0.58–0.69 wt%) in the miarolitic granitic pegmatites. Inclusions of beryl were not observed in clear and transparent axinite-(Mn) crystals and plates under the optical microscope. Increased Be content (180 and 440 ppm) has been also reported in axinite-(Mn) from the Little Three mine (Foord *et al*., 1989). Axinite-(Fe) with high concentration of Be (0.287 *apfu*, 0.62 wt% BeO) was also found in pegmatized granite-aplites from Ziaetdin Mountains, western Uzbekistan (Azimov, 1970). This mineral is characterized by considerable excess B (0.361 *apfu*), the lack of Al^{3+} (0.42 *apfu*) and near stoichiometric Si content. We hypothesize that the increase in Be content is due to Be substitution for basic elements in the axinite structure but further studies are required to confirm.

Besides Be, the most significant impurities in axinite-(Mn) of the Makhan deposit are Sn, Y, and REE and to a lesser degree Sc, Ba, Zn, Ta and Nb (Table 2). The total content of Y and REE is about 0.1 wt% with light REE dominant over heavy REE (L_{REE}/H_{REE} = 3.42). The normalized pattern of REE shows a distinct negative Eu anomaly (Fig. 3). The Mn-Li-Al tourmaline associated with axinite-(Mn) exhibits a similar REE pattern with lower contents of heavy REE (L_{REE}/H_{REE} = 9.6). The normalized pattern of REE in axinite-(Mn) and Mn-Li-Al tourmaline clearly shows the M-type tetrad effect (convex curves) from La to Nd. Such behavior is typical for many granitoid rocks (granitic pegmatites, Li–F granites, ongonites, F-rich rhyolites) and their accessory minerals (apatite, monazite, zircon, tourmaline, lepidolite, spodumene, beryl, garnet, fluorite, cryolite, *etc*.) as reviewed by Peretyazhko & Savina (2010). The negative Eu anomaly is less manifested in quartz, orthoclase and laumontite than in axinite-(Mn) and tourmaline, whereas a weak positive Eu anomaly wais peculiar of adularia. With respect to increasing REE content, the minerals from pockets follow the order adularia < orthoclase < quartz < laumontite < tourmaline < axinite-(Mn). The difference in the contents of REE (except for Eu) between the extremes of this series reach three orders of magnitude. Elevated concentrations of REE in quartz relative to orthoclase and adularia are likely due to the presence of numerous FI (see section 7.2) with unidentified crystalline phases. The high content of Bi (381 ppm, Table 2) in quartz might be a result of microscopic inclusions of native bismuth and/or bismutite. We found that axinite-(Mn) incorporated a majority of rare elements to a greater extent than tourmaline. Overall, comparison of the geochemical features of the two associated borosilicates in pockets indicates that axinite-(Mn) is richer in Be, Sn, REE, Nb, Ta, Hf, Th and U (Table 2). Moreover, axinite-(Mn) from the Malkhan deposit contained more Li, Sn, Nb, Ba, Sc and light REE, but less Cr, Co, Ni, Pb, Th and heavy REE than axinite-(Mn) of the Little Three mine (Foord *et al*., 1989).

Table 1. Chemical composition and structural formulas of axinite-(Mn) and axinite-(Fe) from granitic pegmatites.

	1	2	3	4	5	6	7	8	9	10
SiO_2	42.93	43.10	42.21	42.65	40.64 (0.23)	42.48	41.66	41.66	42.21	41.60
TiO_2	0.24	<0.02	0.28	0.30	0.04 (0.03)		0.01	0.04	0.00	0.00
Al_2O_3	17.37	16.40	17.90	17.00	18.34 (0.11)	18.20	18.00	17.38	17.62	15.78
Fe_2O_3	1.34	2.65	2.28	1.87			0.10			1.20
FeO	2.36	0.70	0.92	1.47	2.80 (0.12)*	3.30*	3.27	12.42*	9.30*	10.80
MnO	9.88	10.02	10.16	11.52	9.94 (0.14)	9.26	11.66	0.43	1.66	2.80
MgO	0.09	0.11	0.03	0.14	0.29 (0.02)	0.50	0.25	0.19	1.29	0.38
CaO	17.99	19.24	17.93	17.43	19.18 (0.13)	18.87	18.08	19.67	19.50	18.20
Na_2O	0.11	0.13	0.16	0.17	<0.03		0.15	0.00		0.12
K_2O	0.19	0.17	0.19	0.18	<0.02		0.02		0.00	0.70
BeO	0.68	0.58	0.69	0.66						0.62
B_2O_3	5.18	4.58	4.96	5.13	6.01 (0.17)	6.21	5.96	6.05**	6.11**	7.10
P_2O_5	0.05	0.09	<0.02	0.04						
H_2O^+	1.63	1.26	1.39				1.26			
H_2O^-	0.04	0.11	0.16				0.04			
$H_2O^{\pm}$				1.09	1.51**	1.46		1.57**	1.58**	0.52
F	0.04	0.03	0.026	<0.02	<0.09				0.00	
$\sum(-O = F_2)$	100.10	99.16	99.28	99.65	98.75 (0.33)	100.28	100.46	99.43	99.27	99.82
					Formula contents per 32 (O,OH) anions					
Si	8.133	8.322	8.083	8.194	8.074	8.013	7.963	7.977	8.009	8.015
Ti	0.034		0.040	0.043	0.006		0.001	0.006		
Al	3.879	3.732	4.040	3.849	4.294	4.046	4.055	3.922	3.940	3.583
$Fe^{3+}_{(Z)}$	0.121	0.268		0.151						0.174
$Fe^{3+}_{(Y)}$	0.070	0.117	0.329	0.119			0.014			
Fe^{2+}	0.374	0.113	0.147	0.236	0.465	0.521	0.523	1.989	1.476	1.740
Mn	1.585	1.639	1.648	1.875	1.673	1.479	1.888	0.070	0.267	0.457
Mg	0.025	0.032	0.009	0.040	0.086	0.141	0.071	0.054	0.365	0.109
Ca	3.652	3.980	3.679	3.588	4.083	3.814	3.703	4.035	3.964	3.757
Na	0.040	0.049	0.059	0.063			0.056			0.045
K	0.046	0.042	0.046	0.044			0.005			0.172
Be	0.309	0.269	0.317	0.305						0.287
B	1.694	1.527	1.640	1.701	2.061	2.022	1.966	2.000	2.001	2.361
Cat. sum	19.964	20.09	20.038	20.208	20.742	20.035	20.245	20.053	20.021	20.700
OH	2.060	1.623	1.776	1.397	2.000	1.837	1.606	2.005	2.000	0.668
O	29.940	30.377	30.224	30.603	30.000	30.163	30.394	29.995	30.000	31.332
An. sum	32	32	32	32	32	32	32	32	32	32

*All Fe is expressed as FeO.**Calculated from stoichiometry. For the sample 5 one-sigma standard deviations are shown in parentheses. Values shown as "<" are below the indicated detection limit. Blank – element not analyzed. Applied analytical methods are wet chemical (samples 1–4, 6, and 7) and electron microprobe (samples 5, 8, and 9). Phosphorus was excluded from calculation of structural formulas because of its small content and position uncertainty in the structure of mineral. $Fe^{3+}_{(Y)} = Fe^{3+}_{(Z+Y)} + Al - 4$ (*apfu*).

1-5–axinite-(Mn) from pockets. 1–4–light-brown crystals, the Sosedka pegmatite body, Malkhan deposit: 1 (Mlh-2939) – crystals on orthoclase, 2 (Mlh-4007G) – crystals on quartz, 3 (Mlh-4002/1) – crystals from loose miarolitic material, 4 (Mlh-4003) – crystals from loose axinite-laumontite aggregate within the "steaming" zone, 5–the Little Three mine, Spessartine dike, California, USA (London *et al*., 2012). 6–10–pocket-free pegmatites: 6–rose, violet-rose axinite-(Mn) from endocontact zone of amazonite-bearing spodumene pegmatite, Eastern Siberia, Russia (Samsonova, 1968); 7–dark grayish-brown axinite-(Mn) pod associated with quartz, K-feldspar, and Fe-rich chlorite, Minnesota, USA (French & Faney, 1972); 8–violet, mostly transparent axinite-(Fe) up to 5 mm in size from iron-contaminated pegmatites at Malešov, Czech Republic (Filip *et al*., 2006); 9–accessory axinite-(Fe) from pegmatites of the O'Grady batholith, Canada (Ercit *et al*., 2003); 10–axinite-(Fe) from pegmatized granite-aplites, Ziaetdin Mountains, Uzbekistan (Azimov, 1970).

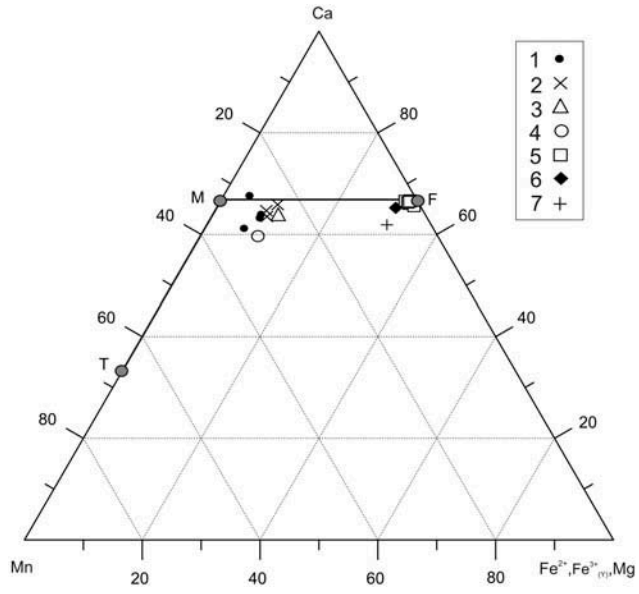

Fig. 2. Composition range of the axinite-group minerals from granitic pegmatites.
End-members: F – axinite-(Fe) $Ca_4Fe_2Al_4B_2Si_8O_{30}(OH)_2$, M – axinite-(Mn) $Ca_4Mn_2Al_4B_2Si_8O_{30}(OH)_2$, and T – tinzenite $(Ca_2Mn_2)Mn_2Al_4B_2Si_8O_{30}(OH)_2$. Miarolitic granitic pegmatites: 1–Sosedka pegmatite body (Table 1, samples 1–4) and 2–Little Three mine (Foord *et al*., 1989; London *et al*., 2012, Table 1, sample 5). Pocket-free granitic pegmatites: 3–Eastern Siberia, Russia (Samsonova, 1968, Table 1 sample 6), 4–Minnesota, USA (French & Faney, 1972, Table. 1, sample 7), 5–Malešov, Czech Republic (Filip *et al*., 2006, Table 1, sample 8), 6–O'Grady batholith, Canada (Ercit *et al*., 2003, Table 1, sample 9), and 7–pegmatized granite-aplites, Ziaetdin Mountains, Uzbekistan (Azimov, 1970, Table 1, sample 10).

6. Cell parameters

Table 3 summarizes unit-cell parameters of axinites from the Malkhan deposit (samples 1–4) and localities not associated with granitic pegmatites (samples 5–7). Malkhan axinite-(Mn) in samples 1–4 shows lower values of *b* (Å) and cell volume (Å^3), but higher β(º) values compared to axinite in samples 5–7. Because no data is available on axinite of other pegmatites, we are not able to conclude whether such cell parameters are specific for all axinites from granitic pegmatites in general or pegmatites of this particular location.

7. Fluid inclusions

Fluid inclusions in quartz and tourmaline from the "A" type pockets of the Malkhan deposit have been widely studied (Peretyazhko *et al*., 2000; Smirnov *et al*., 2000, 2003; Peretyazhko *et al*., 2004a and b; Thomas *et al*., 2012). In contrast, FI in axinite-(Mn) and other minerals of the "B" type pockets have been scarcely investigated (Dmitrieva, 2012). Our work provides important characterization of FI in axinite-(Mn) and associated quartz, orthoclase, adularia, tourmaline and beryl. We define FI as gas-liquid and crystal-fluid inclusions, where the latter may have varying abundances of solid phases. The analysis revealed the presence of primary and secondary or pseudo-secondary FI. The primary FI are spread irregularly in almost all of the minerals. Primary FI occur as scattered clusters irregularly distributed through the entire sample and are not related to cracking of the host mineral. The secondary or pseudo-secondary FI are arranged along linear zones intersecting the grain boundaries, in agreement with criteria established by Roedder (1984). Pseudo-secondary or secondary FI were not considered in this work.

7.1. Morphology and types of fluid inclusions

The size of primary FI varies from 5 to 75 μm, while large FI of 100 μm are sporadic and commonly found in quartz and tourmaline but not in axinite-(Mn) and K-feldspar. Fluid inclusions are variously shaped, including elongated and tubular FI in tourmaline, and irregularly shaped, flattened and rarely rounded FI in axinite-(Mn) and K-feldspar. The tubular FI with well-expressed induction faces are specific to beryl. The following types of FI were identified (Fig. 4).

Type 1. Two-phase inclusions containing aqueous solution and gas bubble (Fig. 4a,b). During cooling, daughter crystals of sassolite sometimes appear in such FI. The crystals are reliably diagnosed using optical properties and Raman spectroscopy (Peretyazhko *et al*., 2000; Smirnov *et al*., 2000). This evidence indicates the presence of boric acid in the FI solution.

Type 2. Three-phase inclusions hosting aqueous boric acid solution, gas bubble and daughter crystal of sassolite (Fig. 4c,d).

Type 3. Multi-phase inclusions containing aqueous solution, gas bubble, and one or more crystalline isotropic and/or anisotropic phases of unknown composition (±sassolite) which occupy 5–20 % of vacuole volume (Fig. 4e). This FI can contain two to five tiny crystals or two to three larger crystals of rounded, irregular and elongated shapes.

Type 4. The inclusions have distorted gas bubble and little fluid and are mainly filled with an entangled-fibrous crystalline aggregate. The crystalline aggregate occurs either as sheaf-like separations and spherules or globules (Fig. 4g,h). The aggregates, similar in appearance to inclusions from minerals of the "A" type pockets, contain topaz, K-feldspar, lepidolite and muscovite, together with boromuscovite, nanpingite and a boron-analogue of nanpingite (Peretyazhko *et al*., 2004a). According to Smirnov *et al*. (2003) and Peretyazhko *et al*. (2004b), type-4 inclusions resemble melt inclusions. Type-4 inclusions are described as specific hydrosilicate inclusions with the unusual behavior of silicate component in melting and subsequent cooling. The inclusions are assumed to capture gel-like water-silicate fluid phases (Peretyazhko *et al*., 2004b; Touret *et al*., 2007; Peretyazhko, 2010; Peretyazhko *et al*., 2010).

Some inclusions were intermediate between FI of type 3 and inclusions of type 4. Such inclusions contained a small

Table 2. Contents of trace elements (in ppm) in minerals from "B" type pockets of the Sosedka pegmatite body determined by ICP-MS.

	Quartz Mlh-4012	Orthoclase Mlh-4007/3	Adularia Mlh-4007/4	Tourmaline Mlh-4006/2	Axinite-(Mn) Mlh-4002/1	Laumontite Mlh-4256
Li	55	458	441			35
Be	0.79	2.82	2.15	5.7	1518	149
Rb	28	4577	5278		5	19
Cs	10.9	578	2154	1.20	8.8	459
Zr	1.67	0.57	0.40	9.2	23	0.72
Hf	0.069	0.024	0.018	0.34	8.5	0.047
Ta	0.37	0.23	0.86	2.92	94	0.90
Nb	0.50	0.16	0.70	1.72	45	0.51
Ba	14.0	8.5	170	34	123	2.09
Sr	1.40	2.41	68	4.36	29	501
Sn	0.26	0.13	0.042	70	1414	0.21
Sb	0.30	6.2	0.14			0.62
Mo	0.068	0.027	0.013	0.37	1.24	0.0074
W	0.11	0.073	0.59			0.18
Pb	2.11	73	42	84	6.6	1.77
Zn	1.97	2.47	2.06	125	195	1.61
Cu	5.9	0.74	1.05	14.2	1.47	3.68
Tl	0.22	27	51	0.24	2.41	0.17
Bi	381	0.44	0.30	2.98	6.5	5.1
Ga	0.67	50	33	292	59	84
Ge	1.53	6.4	8.1	4.43	23	0.46
Th	0.25	0.22	0.51	0.17	5.6	0.39
U	0.14	0.026	0.045	0.066	0.68	0.11
Sc	0.18	0.056	0.037	69	229	0.60
Ni	1.58	0.20	0.27	1.89	1.40	0.14
Co	0.22	0.048	0.020	0.15	0.49	0.076
Cr	0.81	0.12	0.35	1.23	0.87	0.14
V	0.73	0.18	0.13	5.5	47	0.35
Y	1.00	0.79	41	0.38	370	3.47
La	0.24	0.071	0.060	1.68	98	0.29
Ce	0.98	0.16	0.11	5.2	291	0.93
Nd	0.34	0.090	0.046	3.58	208	0.55
Pr	0.077	0.019	0.012	0.90	48	0.12
Sm	0.11	0.054	0.017	1.72	85	0.19
Eu	0.014	0.010	0.011	0.027	1.02	0.024
Gd	0.13	0.066	0.028	0.76	72	0.32
Tb	0.024	0.014	0.0055	0.059	10.5	0.064
Dy	0.14	0.085	0.041	0.24	49	0.39
Ho	0.028	0.016	0.0067	0.036	6.6	0.080
Er	0.084	0.055	0.020	0.084	20	0.25
Tm	0.014	0.011	0.0036	0.020	4.27	0.041
Yb	0.090	0.070	0.027	0.15	43	0.36
Lu	0.016	0.013	0.0036	0.015	8.4	0.059
L_{REE}/H_{REE}	3.32	1.19	1.79	9.60	3.42	1.33

Blank – element not analyzed.

amount of entangled-fibrous or sheaf-like aggregates specific of type 4 inclusions (Fig. 4f). Daughter phases of chlorides were not discovered in FI. In general, the minerals from "B" type pockets predominantly contained type-1 FI. Their volume fraction in quartz and particularly in beryl were reduced due to the increase of FI of types 2 and 3. The FI of type 2 predominated in quartz of the "steaming" zone. The infrequent type-4 inclusions were discovered only in the early growth zones of quartz crystals. The total amount of FI diminished in the zoned crystals of quartz from the early zones to the late ones, while the relative fraction of FI of types 2 and 3 increased.

7.2. Composition and density of solutions in inclusions

We found no evidence of carbon dioxide or other gases during cooling and freezing solutions in FI of all types. However, gas chromatography analysis of minerals from the pockets (axinite-(Mn), adularia, laumontite and beryl) showed that minor amounts of CO_2 (0.03–0.52 rel.%) and CO (0.03–0.11 rel.%) could be present in the water solution from FI (unpublished data; study was performed at the Institute of Earth's Crust, SB RAS Irkutsk). Minor amounts of CO_2, CH_4, H_2S and N_2 were also found in the liquid and gaseous phases of FI

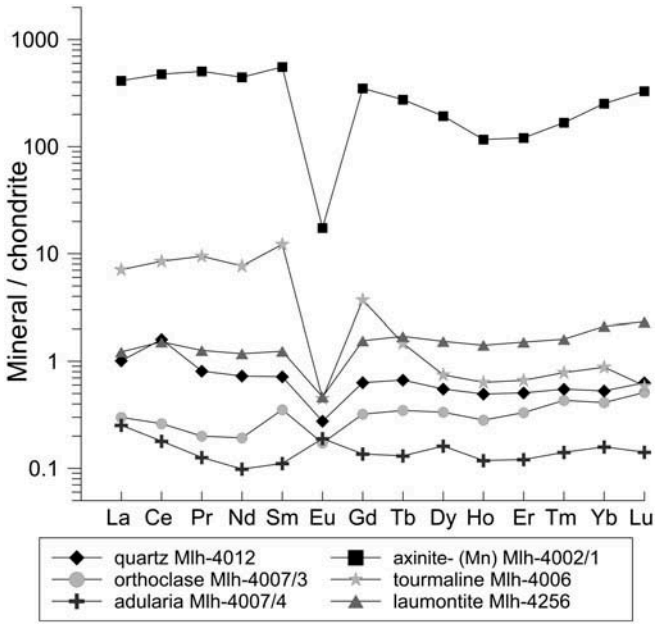

Fig. 3. The REE distribution pattern normalized to chondrite C1 (McDonough & Sun, 1995) in minerals from "B" type pockets.

in quartz from the "A" type pocket by Raman spectroscopy (Peretyazhko *et al.*, 2004a and b). The main anions and cations were HCO_3^-, F^- and Cl^- and K^+, Na^+ and Ca^{2+}, respectively, in aqueous extracts from minerals of the "A" type pockets (Zagorsky & Peretyazhko, 1992). The extracts also contained minor amounts of Mn^{2+}, Fe^{2+}, Mg^{2+} and Li^+. In addition, Raman spectroscopy identified carbonate, bicarbonate and sulfate components in FI from quartz of the "A" type pockets as well as daughter crystal of zabuyelite (Li_2CO_3) in FI from topaz (Thomas *et al.*, 2012). The solutions in FI from minerals of tourmaline-rich miarolitic pegmatites (Peretyazhko *et al.*, 2004a) and synthetic fluid inclusions in the H_3BO_3–NaF–SiO_2–H_2O system modeling mineral-forming processes in pockets of granitic pegmatites (Peretyazhko *et al.*, 2010) might contain aqueous soluble complexes of $[B(OH)_3]°$, $[B(OH)_4]^-$, polyborates $[B_4O_5(OH)_4]^{2-}$, $[B_3O_3(OH)_4]^-$, $[B_5O_6(OH)_4]^-$, fluoroborates $[B_3F_6O_3]^{3-}$, $[BF_2(OH)_2]^-$, $[BF_3(OH)]^-$, and $[BF_4]^-$.

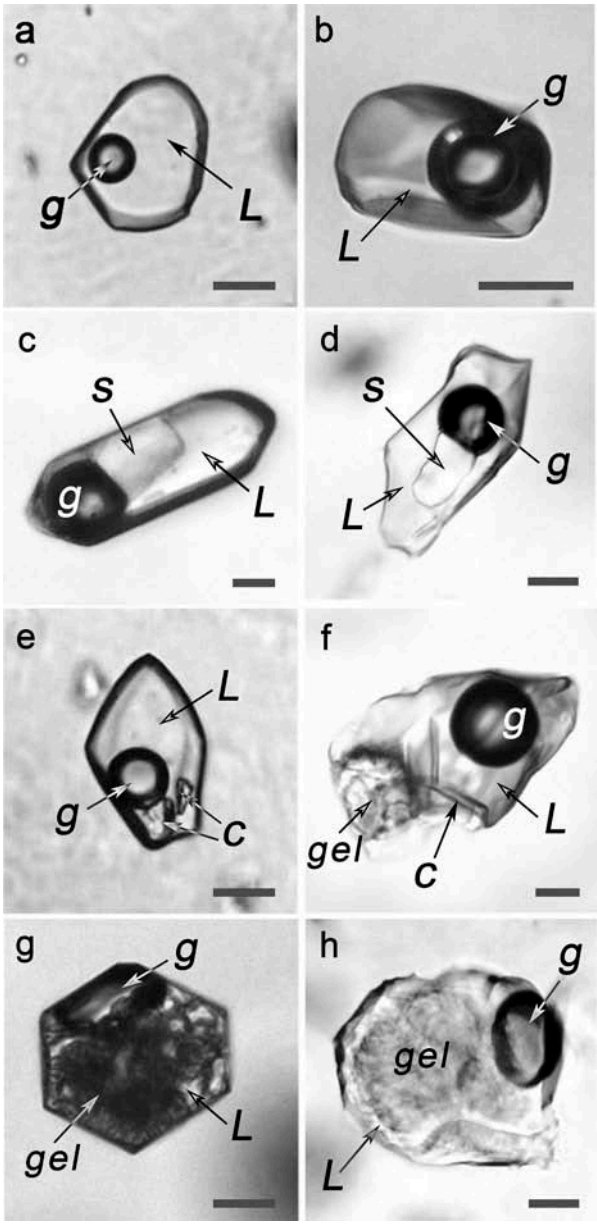

Fig. 4. Types of fluid inclusions.
a) and b) – type 1; c) and d) – type 2; e) – type 3; f) – intermediate between types 3 and 4; g) and h) – type 4.
g – gas, L – liquid, s – sassolite crystal, c – unidentified crystalline phases, and gel – gel-like water-silicate phases. Scale bar is 20 μm.

Table 3. Lattice parameters of axinites.

	Sosedka pegmatite body, Malkhan deposit				Non-pegmatite locations		
	1	2	3	4	5	6	7
a (Å)	7.170(2)	7.167(1)	7.172(1)	7.16(1)	7.162	7.161(4)	7.1703(4)
b (Å)	9.170(3)	9.177(1)	9.178(1)	9.17(1)	9.207	9.213(6)	9.2031(5)
c (Å)	8.977(2)	8.962(1)	8.961(1)	8.96(1)	8.972	8.974(6)	8.9666(4)
α (°)	91.85(2)	91.80(1)	91.86(1)	91.87(1)	91.84	91.80(6)	91.803(4)
β (°)	98.35(2)	98.28(2)	98.31(1)	98.33(1)	98.16	98.11(5)	98.120(4)
γ (°)	77.16(2)	77.19(1)	77.17(1)	77.21(1)	77.34	77.24(5)	77.207(4)
V (Å^3)	569.37(2)	568.78(1)	569.09(1)	567.6(1)	571.4	571.7(4)	571.22(5)

Samples: 1–4–see Table 1; 5–(Belokoneva *et al.*, 1997); 6–(Lumpkin & Ribbe, 1979); 7–(Andreozzi *et al.*, 2004).

Boric acid is a common component of FI in the minerals from Malkhan pegmatites. The concentration of H_3BO_3 reaches 27.5 wt% in the FI solutions (Peretyazhko *et al*., 2000, 2004a), while 53 wt% has also been reported (Thomas *et al*., 2012). Minerals from "B" type pockets contain less H_3BO_3 in FI solutions with C_{H3BO3} ranging from 3.6 to 8.3 wt% (Table 4). The daughter sassolite crystals appeared in some FI of type 1 during the freezing step, whereas it was always present in FI of type 2. Sassolite was a typical phase of FI in quartz (C_{H3BO3} up to 13 wt%) of the "steaming" zone and was also found in some FI in axinite-(Mn) from the "steaming" zone and adularia from the "B" type pockets. However, no FI with sassolite was detected in the orthoclase samples. The results of C_{H3BO3} measurements in FI of the "B" type pocket minerals increase in the order (axinite-(Mn), adularia) < (quartz, beryl) < tourmaline. In addition, C_{H3BO3} was observed to decrease in the external growth zones of some zoned crystals of quartz and beryl.

The salinity ranged from 3.5 to 5.5 wt% NaCl-eq in FI solutions; however, values between 1.6 and 10.5 wt % NaCl-eq. have also been reported (Table 4). The values close to the upper limit (between 7.4 and 9.5 wt% NaCl-eq.) were characteristic of FI solutions in tourmaline. Based on the degree of solution salinity, no regular distinction could be made between FI of different types from axinite-(Mn), adularia, beryl, tourmaline, orthoclase and quartz.

The density of FI solutions ranges between 0.635 and 0.870 g/cm^3 (Table 4). The density values close to the upper limit are typical for orthoclase and adularia (0.825–0.865 g/cm^3), while the values close to the lower limit are typical of beryl and the late growth zones in quartz crystals (0.635–0.753 g/cm^3). We did not detect any substantial difference in the solution density between different types of FI.

7.3. Homogenization temperature of fluid inclusions

The FI of types 1 and 2 were completely homogenized. Homogenization of FI occurred in the liquid phase, with critical phenomena in some cases (the boundary between the liquid and gas phases of FI progressively became unresolvable). Sassolite in FI dissolved at temperatures up to 60°C. The general interval of total homogenization temperature (T_{hom}) was 250–330°C in FI of "B" type pockets minerals (Table 4, Fig. 5). Variation in the homogenization temperature was most significant in quartz (130–380°C) and to lower extent in adularia, and orthoclase (200–340°C), while T_{hom} variation was substantially lower in tourmaline (260–390°C), axinite-(Mn) (285–350°C), and particularly in beryl (300–325°C). Two types of T_{hom} distribution pattern were observed: (1) unimodal (tourmaline, axinite-(Mn) and beryl) and (2) poorly expressed bimodal (quartz, orthoclase and adularia). The first group of minerals had the modal value of 320°C, while the second one had 250–280°C (main) and 310–320°C (minor importance) (Fig. 5).

Inclusions of the types 3 and 4 of ≥ 30 μm size had sassolite and some other crystals decrepitated at temperatures over 350–390°C during heating. The small inclusions (≤10 μm) retained impermeability up to 500°C but some crystals were not dissolved (probably not daughter phases) even after long isothermal exposures close to 450–500°C.

8. Discussion

Formation conditions of axinite have been extensively studied in diverse skarn-ore and skarn-borosilicate deposits. In particular, it has been established that axinite stability is profoundly affected by boron and manganese activities and by the Mn to Fe ratio (Kurshakova, 1968). Axinite-(Mn) and axinite-(Fe) form at high boron activity and the minerals are unstable under low boron and manganese activities. Axinite with different ratios of Mn and Fe of skarn deposits formed over a wide temperature range from 350 to 120°C (Kurshakova, 1968). Fluid inclusions in axinite from the cavities of the Dalnegorsk skarn deposit formed at 450–350°C (Karas & Pakhomova, 2012).

Axinites with variable Mn and Fe contents were synthesized by Nekrasov & Kashirtseva (1975) in the $CaO–Mn(Fe)O–Al_2O_3–SiO_2–B_2O_3$ system at 300–500°C and 0.3–1 kbar. Experimental temperatures and pressures were close to the conditions of post-magmatic stage of miarolitic granitic pegmatite formation. According to experimental data, the upper limit of axinite stability reached 525 ± 10°C (Nekrasov & Kashirtseva, 1975) and the lower limit of stability was < 200°C. Moreover, the stability of axinite has been shown to be substantially affected by B_2O_3 concentration. Increasing B_2O_3 solution concentration from 0.2 to 1.2 mol/l led to increase in the temperature of axinite crystallization from 300°C to 500° C. Further increase of B_2O_3 content up to 1.5 mol/l resulted in crystallization of danburite. Synthesized axinites can concentrate 0.55 wt% Sn at 300°C and up to 0.74 wt% Sn at 500°C (Nekrasov & Kashirtseva, 1975). Note that axinite-(Mn) of the Malkhan deposit also contained a large admixture of Sn (1414 ppm, Table 2).

The content of melt inclusions at the base of quartz crystals growing on the pocket wall begins melting at 500°C (Peretyazhko *et al*., 2004a). This temperature is accepted as an upper temperature limit of hydrothermal mineral formation in pockets of the Malkhan deposit. According to ontogenetic observations, the sequence of mineral formation in the "B" type pockets follows (quartz, orthoclase) → (quartz, Mn-Li-Al-tourmaline ± beryl) → (adularia, axinite-(Mn) ± quartz) → (axinite-(Mn), laumontite) → laumontite.

K-feldspars are usually present as a mixture of monoclinic and triclinic phases (Σt_1 = 0.86–0.96, Δt_1 = 0.23–0.88) in external and internal zones of the Sosedka pegmatite body (Zagorsky, 2012). K-feldspars in the "A" type pockets are triclinic (microcline; Σt_1 = 0.97–0.99, Δt_1 = 0.85–0.93), whereas they are monoclinic in the "B" type

Table 4. Microthermometry of primary fluid inclusions in minerals from "B" type pockets and "steaming" zone of the Sosedka pegmatite body.

Mineral	Type of FI	N	T_{ice},°C	T_{hom},°C	C_{NaCl} eq. (wt.%)	C_{H3BO3} (wt.%)	Density (g/cm^3)
				Minerals from "B" type pockets			
Axinite-(Mn)	1	16	-3.5– -2.3 (–2.9)	285–325 (310)	3.9–5.7 (4.7)	N.f.	0.748–0.765 (0.755)
(1)	3	3	N.d.	320–325 (325)	N.d.	N.f.	N.d.
Adularia	1	63	-5.3– -2.2 (–3.5)	200–335 (270)	3.7–8.3 (5.7)	N.f.	0.784–0.919 (0.825)
(7)	1*	2	–4.1, –5.3	220, 265	6.1, 7.6	3.9, 4.6	0.852, 0.794
	3	4	N.d.	240–315 (280)	N.d.	N.f.	N.d.
	1	9	N.d.	300–320 (300)	N.d.	N.f.	N.d.
Beryl	2	21	-4.6– -2.2 (–2.5)	300–320 (313)	2.4–6.4 (3)	4.3–7.4 (5)	0.685–0.724 (0.703)
(2)	3	6	-5– -2.4 (–4)	300–325 (310)	2.8–7.8 (6.2)	4.0–6.0 (5.2)	0.715–0.800 (0.717)
	1	19	-6.2– -5.3 (–5.7)	260–350 (320)	8.3–9.5 (8.9)	N.f.	0.765–0.782 (0.773)
Tourmaline	2	2	–5.7, –5.3	315, 320	7.4, 7.9	7.5, 8.3	0.698, 0.714
(2)	2*	2	–5.7, –6.1	300, 305	7.9, 8.6	5.1, 7.3	0.746, 0.725
	3	5	–4.9	300–390 (330)	7.7	N.f.	0.770
Orthoclase	1	28	-3.9– -3.1 (–3.5)	220–340 (270)	5.1–6.3 (5.7)	N.f.	0.764–0.885 (0.825)
(5)	3	3	–1.6	220–310 (250)	2.7	N.f.	0.865
	1	105	-3.9– -2 (–3)	160–370 (280)	3.2–6.3 (4.7)	N.f.	0.700–0.944 (0.782)
	2	17	-4.8– -1.6 (–2.9)	180–340 (295)	1.6–7 (3.9)	3.6–6.4 (4.5)	0.635–0.907 (0.742)
Quartz	2*	2	–4.6, –5.4	288, 310	6.6, 7.8	4.5, 6.4	0.719, 0.756
(4)	3	31	-4– -1.8 (–3.5)	200–380 (280)	3.1–6.4 (5.2)	3.4	0.580–0.872 (0.788)
	4	6	N.d.	280–340 (300)	N.d.	N.f.	N.d.
				Minerals from "steaming" zone			
Axinite-(Mn)	1	16	-4.1– -2.8 (–3.4)	305–350 (315)	4.7–6.6 (5.5)	N.f.	0.673–0.759 (0.726)
(1)	2*	2	–3.9, –4.0	299, 313	5.7, 5.8	5.0, 5.2	0.707, 0.737
	3	5	N.d.	320–330 (325)	N.d.	N.f.	N.d.
Quartz	1	26	-7.0– -6.2 (–6.6)	160–360 (285)	9.5–10.5 (10.0)	N.f.	0.762–0.788 (0.775)
(2)	2	25	-6.6– -2.2 (–3.9)	130–355 (250)	2.6–9.5 (5.2)	3.4–13.0 (9.4)	0.583–0.953 (0.824)
	3	4	-4.0– -3.9 (–4.0)	265–330 (295)	5.0–5.2 (5.1)	11.6–12.8 (12.2)	0.694–0.785 (0.740)

*Measurements of fluid inclusions were performed by S.Z. Smirnov (Institute of Geology and Mineralogy SB RAS, Novosibirsk). In parentheses after the mineral – is the number of analyzed samples. N – quantity of FI. In brackets after values of T_{ice}, T_{hom}, C_{NaCl} eq., C_{H3BO3} and Density – are average values. N.d. – no data. N.f. – sassolite not found.

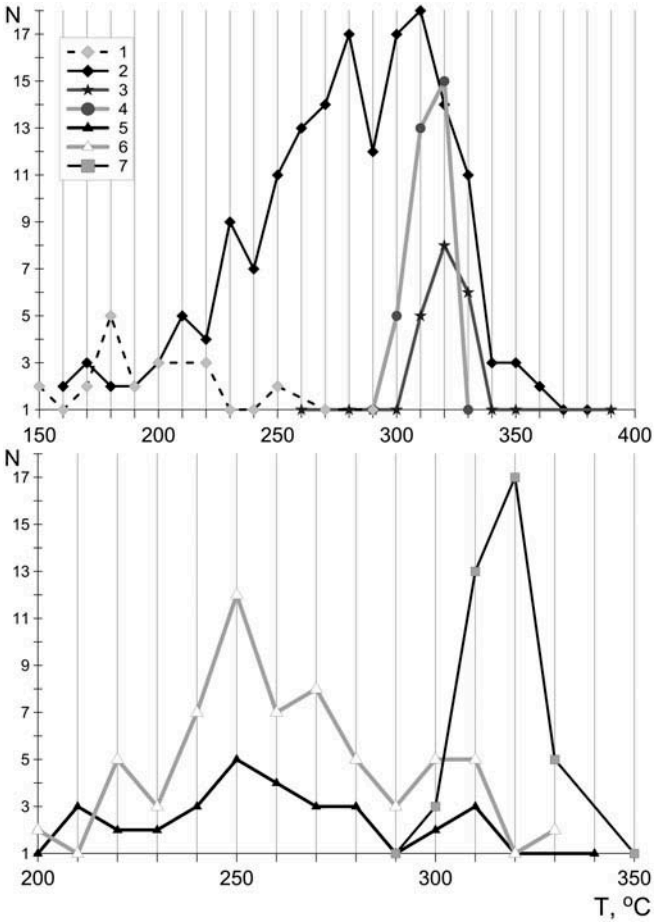

Fig. 5. The homogenization temperature (T_{hom}) ranges of fluid inclusions in minerals from axinite-(Mn)-bearing pockets.
The numbers are defined as following: 1–K-feldspar from pocket-hosting pegmatite, while 2–7–minerals from pockets including 2–quartz, 3–tourmaline, 4–beryl, 5–orthoclase, 6–adularia, and 7–axinite-(Mn).

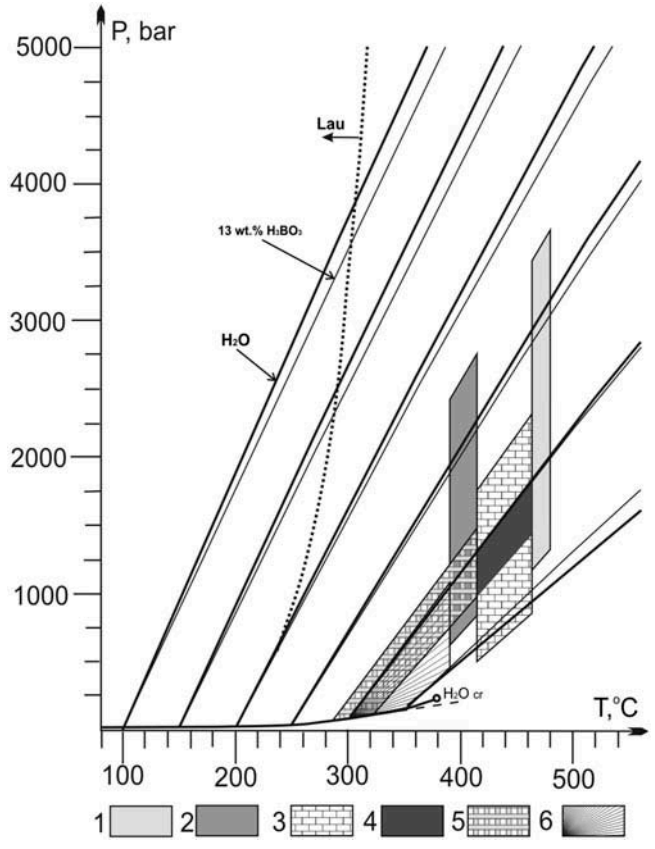

Fig. 6. Vapor–liquid curves and isochores of the H_2O–H_3BO_3 system.
Isochores for H_2O (thick lines) and fluids with 13 wt.% H_3BO_3 (thin lines) are obtained from the homogenization temperatures 100–350°C after Peretyazhko & Zagorsky (2002) and Peretyazhko *et al*. (2004a). The dashed line shows the position of univariant curve in *P-T* diagram obtained from Chipera & Apps (2001) experimental data for the reaction: laumontite (Lau) ⇔ wairakite + $2H_2O$. H_2O cr – critical point of pure water. Marked areas *P-T* conditions of mineral formation in axinite-containing pockets according to data on K-feldspar geothermometers and fluid inclusions in minerals (Table 4): 1–orthoclase, 2–adularia, 3–tourmaline, 4–beryl, 5–axinite-(Mn), and 6–axinite-(Mn) from "steaming" zone.

pockets (orthoclase and adularia; Σt_1 = 0.79–0.83). The adularia has a more regular structure with smaller *a* unit-cell parameter than the orthoclase. In the "steaming" zone and "C" type pockets both orthoclase and microcline were found. The microcline from "C" type pockets is characterized by a lower degree of triclinic ordering (Δt_1 = 0.16–0.20) as compared with microcline of the "steaming" zone (Δt_1 = 0.59–0.82). Variable content of impurity elements (Rb, Cs and Ba) in K-feldspars and conditions of crystallization (pH of fluid) might explain the formation of metastable orthoclase and adularia instead of stable microcline in pockets of different type (Zagorsky, 2012).

The results of the fluid-inclusion study alone were not sufficient to conclusively determine the temperature of mineral formation in the pockets. The total homogenization temperature of FI did not correspond to the temperature of inclusion capture as shown by the observation that quartz in pocket-hosting pegmatite matrix had lower T_{hom} than quartz and other minerals from pockets. The observation was also supported by higher T_{hom} of FI in axinite-(Mn) than in the earlier-formed orthoclase (Fig. 5) and by significant departure of T_{hom} from the temperatures obtained with K-feldspar geothermometers.

Fluid pressure in pockets was evaluated using isochores of the H_2O–H_3BO_3 system (Peretyazhko & Zagorsky, 2002; Peretyazhko *et al*., 2004a) corresponding to T_{hom} of FI and accepted temperatures of mineral formation (Fig. 6). K-feldspar geothermometers showed that temperatures of K-feldspar formation were 510–500°C for external and internal zones of the Sosedka pegmatite body, 480–465°C for orthoclase of early generation in pockets and 415–390°C for adularia (Zagorsky, 2012). The 415–390°C temperature interval was particularly important, because this temperature range could allow formation of axinite-(Mn) together with adularia. In addition, tourmaline and beryl formation temperatures were within the temperature interval of 465–415°C corresponding to orthoclase and adularia formation.

The temperature ranges (Fig. 6) are in agreement with the expected *P-T* areas of FI formation in orthoclase, adularia, tourmaline, beryl and axinite-(Mn) from pockets and the "steaming" zone. Fluid inclusions in orthoclase were captured at fluid pressures ranging from 3.4–3.7 to 1.3 kbar as determined from isochores for aqueous solutions with <13 wt% H_3BO_3 at T_{hom} of 220 and 340°C. For adularia the fluid pressure ranged from 2.5–2.8 to 0.6–0.8 kbar (isochores at T_{hom} of 200 and 335°C). Fluid inclusions in tourmaline formed at pressure from 2.3–1.8 to 0.9–0.5 kbar and temperature of 465–415°C (isochores at T_{hom} of 260 and 390°C), and in beryl from 1.8–1.5 to 0.6–0.8 kbar (isochores at T_{hom} of 220 and 335°C). The lower temperature limit of crystallization of axinite-(Mn) in the "B" type pockets is expected to be higher than T_{hom} in FI (285–325°C) and the upper limit lower than 415°C (maximum temperature of adularia formation). Fluid inclusions in axinite-(Mn) of "B" type pockets were captured at pressures from 1.5–1 to 0.2–0.1 kbar and at 415–285°C. Fluid inclusions in axinite-(Mn) of the "steaming" zone without adularia could form over the temperature range from 390°C to T_{hom} (350–305°C) and a pressure from 1–0.5 to 0.2–0.1 kbar. According to ontogenetic observations, axinite-(Mn) crystallized both before and together with laumontite in the "steaming" zone. Simultaneous crystallization of laumontite and axinite-(Mn) at fluid pressure <1 kbar should occur at temperatures below 250–230°C (upper limit of laumontite stability according to Chipera & Apps (2001), Fig. 6). We did not find fluid inclusions in axinite-(Mn) with T_{hom} < 305–285°C, presumably because FI were not captured in the low-temperature conditions of axinite-(Mn) crystallization.

Analysis of FI data revealed that mineral crystallization in the "B" type pockets occurred with considerable variations of fluid pressure (Fig. 6). An abrupt drop of fluid pressure indicated rupture of pockets characteristic of many miarolitic granitic pegmatites in different regions of the world (Foord *et al*., 1989; Miarolitic Pegmatites, 1999; Peretyazhko *et al*., 1999; 2004a; Peretyazhko, 2009, 2010). Repeated pressure drops in the adiabatic regime resulted in oscillatory temperature variations accompanied by gradual reduction of pocket formation. The formation of the "steaming" zone might be a consequence of the rupture of axinite–adularia pockets of the "B" type in the Sosedka pegmatite body.

It should be noted that *P-T* conditions of mineral formation estimated for the "B" type pockets could not be extended to other types of pockets. Sharp distinctions in mineral composition of miarolitic material indicate that fields of mineral stability differed markedly in various pockets and depended on pH fluids. Tourmalines have been shown to form in the presence of boric acid predominantly in acidic or neutral aqueous solutions (Morgan & London, 1989; and the reviews of Peretyazhko *et al*., 2000, and London, 2011), while zeolites formed in highly alkaline solutions (Senderov & Khitarov, 1970; Barrer, 1985). According to Setkova *et al*. (2009), Li-Al tourmaline (elbaite) was unstable in alkaline conditions when NaOH was added to boric acid solution at 450–750°C and 1–1.5 kbar.

Increasing alkalinity of mineral-forming fluids favors the crystallization of Si-poor zeolites (laumontite instead of stilbite). We show that laumontite is a predominant mineral in the "B" and "C" type pockets while stilbite occurs only in some "A" type pockets. Adularia is stable in poorly or moderately alkaline fluids and, as a result, it occupies an intermediate position between tourmaline and zeolites. A close association of axinite-(Mn) with adularia in "B" type pockets and with datolite and danburite in skarn-borosilicate deposits (Kurshakova, 1976) provides evidence of axinite formation in heightened-alkalinity mineral-forming fluids.

Alkalinity of mineral-forming fluids increased in the series of "A", "B" and "C" type pockets, corresponding to the increased intensity of Li-Al tourmaline corrosion and its transformation into asbestiform tourmaline (Fig. 1d). The fluid alkalinity substantially affected the stability of Li-Al tourmaline (pinkish red rubellite) while the preceding and the following generations of Mn-Li-Al dark-brown or black tourmaline did not change. The long-term mining operations of the Sosedka pegmatite body showed that adularia, axinite-(Mn) and laumontite were reliable indicators of unfavorable conditions for gem-tourmaline appearance in pockets (Zagorsky, 2015).

The fluid pressure drop was accompanied by replacement of orthoclase by adularia with increased content of Ba, Sr, Rb and Cs in the Sosedka body (Zagorsky, 2012, 2015) and in Amazonitovaya pegmatite vein of the Kukurt gemstone cluster in the Pamirs (Peretyazhko *et al*., 1999). The Rb/Cs ratio sharply decreased with pressure decrease in the adularia of both pegmatites with respect to the earlier orthoclase, indicating the rise of alkalinity and enrichment of Cs of residual mineral-forming fluids in pockets.

The change of acidity-alkalinity in aqueous solutions leads to change in boron-oxygen coordination. Peretyazhko *et al*. (2000) provided an overview of behavior of boric acid solutions and diverse boron-oxygen, boron-fluorine and hydroxy-fluorine-boron complexes under hydrothermal conditions *versus* pH, boron concentration, temperature and presence of different salts in fluids. The hydrated boron acid molecule forms tetraborate and polyborate complexes. Instability of H_3BO_3 in mineral-forming fluids of heightened alkalinity (pH > 7) might explain the low concentrations of boric acid (up to 5.2 wt%) in the FI solution in adularia and axinite-(Mn) from "B" type pockets with respect to minerals in the "A" type pockets.

9. Conclusions

Axinite-(Mn) was found in miarolitic granitic pegmatites of the Malkhan gem-tourmaline deposit. The mineral occurs in the pockets in which Li-Al tourmaline (rubellite) was either absent or transformed into aggregates of asbestiform tourmaline. Axinite-(Mn) is associated with quartz,

orthoclase, adularia and laumontite. The pockets may also contain dark, corroded Mn-Li-Al tourmaline and colorless or pale-pink beryl. The mineral association with axinite-(Mn) was formed from low-salinity (1.6–10.5 wt% NaCl-eq.), B-containing fluids (up to 13 wt% H_3BO_3) of heightened alkalinity at temperatures less than 415°C and fluid pressures lower than1.5 kbar. The axinite-(Mn) contains high concentrations of trace elements, *e.g.* Be, Sn, REE, Nb, Ta, Hf, Th and U. The axinite-(Mn) + adularia ± laumontite association is an indicator of unfavorable conditions for the occurrence of gem tourmalines in miarolitic granitic pegmatites. Axinite is an exotic accessory mineral in granitic pegmatites because conditions favorable for axinites formation are seldom reached.

Acknowledgements: We are grateful to G.A. Pogudina, E.V. Kaneva and S.Z. Smirnov for performing wet chemical analysis, X-ray diffraction and additional fluid-inclusion study, respectively. We thank the anonymous reviewers and chief editor S.V. Krivovichev for valuable comments and suggestions that helped to improve the quality of the manuscript. We regret to inform that, during preparation of the manuscript, the leading author Dr. V.Ye. Zagorsky passed away after a long illness.

References

Albertini, C. (1983): Famous mineral localities: Baveno, Italy. *Mineral. Record*, **14**, 157–168.

Andreozzi, G.B., Lucchesi, S., Graziani, G. (2000): Structural study of magnesioaxinite and its crystal-chemical relations with axinite-group minerals. *Eur. J. Mineral.*, **12**, 1185–1194.

Andreozzi, G.B., Lucchesi, S., Graziani, G., Russo, U. (2004): Site distribution of Fe^{2+} and Fe^{3+} in the axinite mineral group: New crystal-chemical formula. *Am. Mineral.*, **89**, 1763–1771.

Azimov, P.T. (1970): Beryllium-containing axinite from pegmatized granite-aplites in Ziaetdin Mountains, western Uzbekistan. *Uzbek. Geol. Zhurn.*, **14**, 21–23. (in Russian).

Barrer, V. (1985): Hydrothermal chemistry of zeolites. Mir, Moscow, 420 p (in Russian).

Barsanov, G.P. (1961): On isomorphous series of axinite and new mineral species – severgenite. *Proc. Mineral. Museum*, **3**, 10–18. (in Russian).

Belokoneva, E.V., Pletnev, P.A., Spiridonov, E.M. (1997): On crystal structure of low-manganese tinzenite (severginite). *Cristallografia*, **42**, 1010–1013. (in Russian).

Belokoneva, E.L., Goryunova, A.N., Pletnev, P.A., Spiridonov, E. M. (2001): Crystal structure of high-manganese tinzenite from the Falotta deposit in Switzerland. *Crystallogr. Rep.*, **46**, 30–32.

Bruker AXS. (2008): TOPAS V4: general profile and structure analysis software for powder diffraction data. Bruker AXS Inc., Karlsruhe, Germany.

Bukanov, V.V. (2014): Gemstones and collection minerals. Encyclopedia, St.-Petersburg, 464 p. (in Russian).

Chipera, S.J. & Apps, J.A. (2001): Geochemical stability of natural zeolites. *in* "Natural Zeolites: Occurrence, Properties, Applications", D.L. Bish and D.W. Ming, eds. *Rev. Mineral. Geochem.*, Mineralogical Society of America, Blacksburg, Virginia, USA, 117–161.

Deer, W.A., Howie, R.A., Zussman, J. (1997): Rock-forming minerals. **1B**, Disilicates and Ring silicates, 3rd edition. Longman, London.

Dmitrieva, A.S. (2012): Fluid inclusions in minerals from pockets with different mineralization in pegmatites of the Malkhan deposit. *in* "Modern problems of geology, geochemistry and geoecology of russian far east: materials of the 4th regional conference of young researches", A.I. Khanchuk, ed. Vladivostok, Dal'nauka, 95–98. (in Russian).

Ercit, T.S., Groat, L.A., Gault, R.A. (2003): Granitic pegmatites of the O'Grady batholith, N.W.T., Canada: a case study of the evolution of the elbaite subtype of rare-element granitic pegmatites. *Can. Mineral.*, **41**, 117–137.

Fersman, A.E. (1960): Selected works (7 volumes). Publishing House of the USSR Academy, Moscow, **6**, 742 p. (in Russian).

Filip, J., Kolitsch, U., Novák, M., Schneeweiss, O. (2006): The crystal structure of near-end-member ferroaxinite from an iron-contaminated pegmatite at Malesov, Czech Republic. *Can. Mineral.*, **44**, 1159–1170.

Foord, E.E., Spaulding, L.B, Jr, Mason, R.A., Martin, R.F. (1989): Mineralogy and paragenesis of the Little Three mine pegmatites, Ramona district, San Diego County, California. *Mineral. Record*, **20**, 101–127.

French, B.M. & Faney, J.J. (1972): Manganaxinite from the Mesabi range, Minnesota. *Am. Mineral.*, **57**, 989–992.

Grew, E.S. (1996): Metamorphic borosilicates and boron in metamorphic minerals. *in* "Boron: Mineralogy, Petrology and Geochemistry", E.S. Grew and L.M. Anovitz, eds., *Rev. Mineral.*, Mineralogical Society of America, **33**, 387–502.

Janeczek, J. (2007): Intragranitic pegmatites of the Strzegom-Sobótka massif – an overview. *Granitoids in Poland, Am. Mineral. Monogr.*, **1**, 193–201.

Karas, O.A. & Pakhomova, V.A. (2012): Fluid regime of the Dalnegorsk boron-rich lime-skarn deposit formation (the Primorsky Region, Russia). *Zapiski RMO (Proceedings of the Russian Mineralogical Society)*, Vol. CXLI, **6**, 18–28. (in Russian).

Kurshakova, L.D. (1968): Composition and paragenesis of axinite. *in* "Metasomatism and others questions of physic-chemical petrology". Nauka, Moscow, 289–311. (in Russian).

Kurshakova, L.D. (1976): Physico-chemical conditions of skarn-borosilicate deposits. Nauka, Moscow, 274 p. (in Russian).

London, D. (2011): Experimental synthesis and stability of tourmaline: a historical overview. *Can. Mineral.*, **49**, 117–136.

London, D., Morgan, G.B., Paul, K.A., Guttery, B.M. (2012): Internal evolution of miarolitic granitic pegmatites at the Little Three mine, Ramona, California, USA. *Can. Mineral.*, **50**, 1025–1054.

Lumpkin, G.R. & Ribbe, P.H. (1979): Chemistry and physical properties of axinites. *Am. Mineral.*, **64**, 635–645.

McDonough, W.E. & Sun, S. (1995): The composition of the Earth. *Chem. geol.*, **120**, 223–253.

Miarolitic Pegmatites (1999): Zagorsky, V.Ye., Peretyazhko, I.S., and Shmakin, B.M.: Granitic pegmatites, **V.3**. Nauka, Novosibirsk, 488 p. (in Russian).

Minerals. Handbook (1981): **V. 3**, Issue 2. Kurshakova, L.D., Chukhrov, F.V., Smolyaninova, N.N., eds. Nauka, Moscow, 211–227 (in Russian).

Morgan, G.B. & London, D. (1989): Experimental reactions of amphibolite with boron-bearing aqueus fluids at 200 Mpa: implications for tourmaline stability and partial melting in mafic rocks. *Contr. Mineral. Petrol.*, **102**, 281–297.

Nekrasov, I.Ya. & Kashirtseva, G.A. (1975): Conditions of hydrothermal synthesis of tin-bearing axinite. *Dokl. Akad. Nauk*., **222**, 440–443. (in Russian).

Ozaki, M. (1972): Chemical composition and occurrence of axinite. *Kumamoto J. Sci. Geol*., **9**, 1–34.

Peretyazhko, I.S. (2009): Inclusions of magmatic fluids: PVTX properties of aqueous salt solutions of various types and petrological implications. *Petrology*, **17**, 178–201.

Peretyazhko, I.S. (2010): Genesis of mineralized cavities (miaroles) in granite pegmatites and granites. *Petrology*, **18**, 183–208.

Peretyazhko, I.S. & Savina, E.A. (2010): Tetrad effects in the rare earth element patterns of granitoid rocks as an indicator of fluoride-silicate liquid immiscibility in magmatic systems. *Petrology*, **18**, 514–543.

Peretyazhko, I.S. & Zagorsky, V.Ye. (2002): The influence of H_3BO_3 on fluid pressure in granitic pegmatite miaroles: a computation of isochors and the density of boric solutions. *Dokl. Earth Sci*., **383A**, 340–345.

Peretyazhko, I.S., Zagorsky, V.Ye., Prokof'ev, V.Yu., Gantimurova, T.P. (1999): Miarolitic pegmatites of the Kukurt group of gemstone deposits, central Pamirs: the evolution of physical conditions in the Amazonitovaya vein. *Geochem. Int*., **37**, 108–127.

Peretyazhko, I.S., Prokof'ev, V.Yu., Zagorsky, V.Ye., Smirnov, S.Z. (2000): Role of boric acids in the formation of pegmatite and hydrothermal minerals: petrologic consequences of sassolite (H_3BO_3) discovery in fluid inclusions. *Petrology*, **8**, 214–237.

Peretyazhko, I.S., Zagorsky, V.Ye., Smirnov, S.Z., Mikhailov, M.Y. (2004a): Conditions of pocket formation of the Oktyabrskaya tourmaline-rich gem pegmatite (the Malkhan field, Central Transbaikalia, Russia). *Chem. Geol*., **210**, 91–111.

Peretyazhko, I.S., Smirnov, S.Z., Thomas, V.G., Zagorsky, V.Ye. (2004b): Gels and melt-like gels in high-temperature endogeneous mineral formation. *in* "Metallogeny of the Pacific Northwest: tectonics, magmatism and metallogeny of active continental margins", A.I. Khanchuk, G.A. Gonevchuk, A.N. Mitrokhin, L.F. Simanenko, N.J. Cook, R. Seltmann, eds. Vladivostok, Dal'nauka, 306–309.

Peretyazhko, I.S., Smirnov, S.Z., Kotel'nikov, A.R., Kotel'nikova, Z.A. (2010): Experimental study of the system H_3BO_3–NaF–SiO_2-H_2O at 350–800ºC and 1–2 kbar by the method of synthetic fluid inclusions. *Russ. Geol*. *Geophy*, **51**, 349–368.

Roedder, E. (1984): Fluid Inclusions. *Reviews in Mineralogy*, **12**. Mineralogical Society of America, Blacksburg, Virginia, USA, 644 p.

Samsonova, N.S. (1968): Axinite from spodumene pegmatites (Eastern Siberia). *Proc. Mineral. Mus*., **18**, 225–227. (in Russian).

Sanero, E. & Gottardi, G. (1968): Nomenclature and crystal chemistry of axinites. *Am. Mineral*., **53**, 1407–1411.

Senderov, E.E. & Khitarov, N.I. (1970): Zeolites, their synthesis and conditions of formation in nature. Nauka, Moscow, 283 p. (in Russian).

Setkova, T.V., Shapovalov, Yu.B., Marakushev, A.A., Balitskii, V. S. (2009): Experimental study of stability and crystallization peculiarities of tourmaline in hydrothermal conditions. *Dokl. Earth Sci*., **425**, 490–493.

Smirnov, S.Z., Peretyazhko, I.S., Prokof'ev, V.Yu., Zagorsky, V.Ye., Shebanin, A.P (2000): The first finding of sassolite (H_3BO_3) in fluid inclusions in minerals. *Russ. Geol. Geophys*, **41**(2), 193–205.

Smirnov, S.Z., Peretyazhko, I.S., Zagorsky, V.Ye., Mikhailov, M. Yu. (2003): Inclusions of unusual late magmatic melts in quartz from the Oktyabr'skaya pegmatite vein, Malkhan field (Central Transbaikal Region). *Dokl. Earth Sci*., **392**, 999–1003.

Thomas, R., Davidson, P., Badanina, E. (2012): Water- and boron-rich melt inclusions in quartz from the Malkhan pegmatite, Transbaikalia, Russia. *Minerals*, **2**, 435–458.

Touret, J.L.R., Smirnov, S.Z., Peretyazhko, I.S., Zagorsky, V.Ye., Thomas, V.G. (2007). Magmatic-hydrothermal transition in tourmaline-bearing miarolitic pegmatites: Hydrosaline Fluids or Silica Gels? *International Symposium. Granitic Pegmatites: The State of the Art, Porto, Portugal*, 92–93.

Zagorsky, V.Ye. (2010): Malkhan gem tourmaline deposit: types and nature of miaroles. *Dokl. Earth Sci*., **431**, 314–317.

Zagorsky, V.Ye. (2012): Mineralogy of pockets of the Malkhan tourmaline deposit (Transbaikalia): Feldspars of the Sosedka Vein. *Russ. Geol. Geophys*, **53**, 522–534.

Zagorsky, V.Ye. (2015): Sosedka pegmatite body at the Malkhan gem tourmaline deposit, Transbaikalia: composition, inner structure, and petrogenesis. *Petrology*, **23**, 68–92.

Zagorsky, V.Ye. & Peretyazhko, I.S. (1992): Gem pegmatites of Central Transbaikalia. Nauka, Novosibirsk, 224 p. (in Russian).

Zagorsky, V.Ye. & Peretyazhko, I.S. (2008): The Malkhan gem tourmaline deposit in Transbaikalia, Russia. *Mineralogical Almanac*, **13b**, 4–39.

Zagorsky, V.Ye. & Peretyazhko, I.S. (2010): First $^{40}Ar/^{39}Ar$ Age determinations on the Malkhan granite–pegmatite system: geodynamic implications. *Dokl. Earth Sci*., **430**, 172–175.

Zagorsky, V.Ye., Peretyazhko, I.S., Sapozhnikov, A.N., Zhukhlistov, A.P., Zvyagin, B.B. (2003): Borocookeite, a new member of the chlorite group, from the Malkhan gem tourmaline deposit, Central Transbaikalia, Russia. *Am. Mineral*., **88**, 830–836.

Received 19 June 2015
Modified version received 18 December 2015
Accepted 4 April 2016